ELSEVIER

Chemical Engineering Journal 140 (2008) 101–109

Chemical Engineering Journal

www.elsevier.com/locate/cej

Simulation of heterotrophic storage and growth processes in activated sludge under aerobic conditions

Bing-Jie Ni, Han-Qing Yu *

School of Chemistry, University of Science & Technology of China, Hefei 230026, China

Received 2 June 2007; received in revised form 11 September 2007; accepted 12 September 2007

Abstract

In this work, an extension of the Activated Sludge Model No. 3 (ASM3) is presented which takes oxygen transfer, microbial maintenance, and biomass decay into account, in order to describe the heterotrophic storage and growth processes in activated sludge. The sensitivity of the effluent chemical oxygen demand and oxygen uptake rate to the stoichiometric and kinetic coefficients was analyzed. Model calibration was successfully performed by comparing measured and predicted values for model components. Thereafter, the model was evaluated with the experimental results of four independent case studies. Results show that the established model is able to better and mechanistically describe the heterotrophic storage and growth processes in activated sludge.

Keywords: Activated sludge; Activated Sludge Model No. 3 (ASM3); Chemical oxygen demand (COD); Growth; Modeling; Oxygen uptake rate (OUR); Storage

1. Introduction

Mathematical modeling is useful exercise for understanding and optimizing substrate utilization by microorganisms in complex systems. Model simulations can provide a solid foundation for design and operation of various biological treatment systems. For the activated sludge process, modeling has gained significant popularity in the past decades. The activated sludge model suite established by the International Water Association Task Group [1] has provided a standardized set of basic models for biological wastewater treatment processes. These models have been widely accepted in the scientific community and used by the environmental engineers. It has evolved from a simple growth-based kinetics model, Activated Sludge Model No. 1 (ASM1) [2], to a more complicated model involving the description of storage phenomena, i.e., Activated Sludge Model No. 3 (ASM3) [3].

The ASM1 was developed primarily for municipal treatment plants using activated sludge process to describe the removal of organic carbon and ammonium-N. The subsequent ASM3 [1,3] was established for overcoming a number of shortcomings that have emerged from its applications, focusing on biological N removal [4]. The main reason behind such a shift is the increasing understanding on the important role of storage polymers as an essential intermediate in the overall substrate removal by activated sludge, in particular when activated sludge is alternatively subjected to feast and famine conditions [5–7].

However, when ASM3 is used to interpret the data obtained in short-term respirometric batch experiments, inconsistencies often arise [5]. In order to keep the modeling simple [3], in ASM3 it is assumed that all readily biodegradable substrate is initially stored as internal storage products before it is used for growth at the famine phase. However, this is not true in many cases. Krishna and van Loosdrecht [5] found that ASM3 was not appropriate in two cases: one was the discontinuity in the biomass growth rate observed experimentally at feast and famine phases, while another was that it required prediction of a higher level of internal storage polymers than the measured to fit the oxygen consumption. In actual situations storage and growth occur simultaneously at the feast phase, as opposed to the assumption of ASM3, in which only storage occurs at the feast phase [5]. Thus, it was suggested that the simultaneous storage and growth should be taken into account for a better interpretation of the experimental results [5]. Thus, it becomes clear that ASM3 should be extended to account for the simultaneous storage and growth occurring in activated sludge.

Therefore, in this work a generalized model considering simultaneous storage and growth processes in activated sludge

* Corresponding author. Tel.: +86 551 3607592; fax: +86 551 3601592.
E-mail address: hqyu@ustc.edu.cn (H.-Q. Yu).

1385-8947/$ – see front matter © 2007 Elsevier B.V. All rights reserved.
doi:10.1016/j.cej.2007.09.017

under aerobic conditions is established. In this model oxygen transfer, microbial maintenance, and biomass decay are all taken into account. A sensitivity analysis on the model parameters is performed to gain a better insight into the model structure. This model is verified by comparing the experimental and simulating results for four independent case studies. It is expected that the information provided in this work will be useful to improve our understanding on the storage and growth processes in activated sludge.

2. Model development

The ASM3 model was modified to introduce simultaneous substrate storage and growth concept, considerations of microbial maintenance processes, and oxygen transfer. This extension of ASM3 model is structured with seven model components or state variables, including dissolved oxygen (DO), S_O; readily biodegradable substrate, S_S; ammonia, S_{NH_4}; slowly biodegradable substrate, X_S; heterotrophic biomass, X_H; particulate inert COD, X_I; and storage products of active heterotrophic biomass, X_{STO}. The model considers seven microbial processes: hydrolysis of slowly biodegradable substrate, growth on readily biodegradable substrate, aerobic storage of readily biodegradable substrate, growth on storage products, maintenance on readily biodegradable substrate, maintenance on storage products, biomass decay, and oxygen transfer. Related process kinetics and stoichiometry describing the interactions and transformations among model components are expressed in a way that is compatible with previous mathematical models for formulating biochemical reactions of activated sludge [1–3].

The structure of the proposed model is presented in a matrix format [1] reflecting the basic stoichiometric relationships constituting the backbone of the model. The matrix format is outlined in Table 1, where model components are listed in the upper row; the rightmost column gives the process rate expressions; the relevant stoichiometric coefficients are incorporated in appropriate matrix cells. In this way, the rate of change (generation or utilization) in a model component for a given biochemical process is obtained by multiplication of related process stoichiometrics and kinetics [8].

A schematic framework is illustrated in Fig. 1 to describe the relationships among the different groups of components of the model. In this framework, the slowly biodegradable substrate in wastewater is first hydrolyzed to readily biodegradable substrate by the heterotrophs. The biomass can use it for simultaneous storage and growth. When the readily biodegradable substrate is depleted (as low as the half saturation concentration for the primary growth), the degradation (secondary growth) of the storage polymers takes place. In addition to growth, microbial maintenance on the external (S_S) and internal (X_{STO}) substrate is also an important compartment in this integrated model for describing storage and growth processes in activated sludge. Finally, biomass is subjected to decay and produces inert organic carbon.

As shown in Fig. 1, the simultaneous microbial storage and growth concept [9–10] is incorporated into the model in this work. This concept can be explained in such a way that the heterotrophs are capable of simultaneously storing the external

Table 1
Stoichiometric and kinetic matrix for the developed model

Process	Component							Kinetics rates expressions
	S_O O_2	S_{NH_4} N	S_S COD	X_I COD	X_S COD	X_H COD	X_{STO} COD	
1. Hydrolysis			1		−1			$k_H \frac{X_S/X_H}{K_X+(X_S/X_H)} X_H$
2. Storage	$-\frac{1-Y_{STO}}{Y_{STO}}$		$-\frac{1}{Y_{STO}}$				1	$k_{STO} \frac{S_S}{K_S+S_S} \frac{S_O}{K_O+S_O} X_H$
3. Growth on S_S	$-\frac{1-Y_{H,S}}{Y_{H,S}}$	$-i_{NBM}$	$-\frac{1}{Y_{H,S}}$			1		$\mu_{H,S} \frac{S_S}{K_S+S_S} \frac{S_O}{K_O+S_O} \frac{S_{NH_4}}{K_{NH_4}+S_{NH_4}} X_H$
4. Growth on X_{STO}	$-\frac{1-Y_{H,STO}}{Y_{H,STO}}$	$-i_{NBM}$				1	$-\frac{1}{Y_{H,STO}}$	$\mu_{H,STO} \frac{K_S}{K_S+S_S} \frac{S_O}{K_O+S_O} \frac{S_{NH_4}}{K_{NH_4}+S_{NH_4}} \frac{X_{STO}/X_H}{K_{STO}+(X_{STO}/X_H)} X_H$
5. Maintenance on S_S	−1		−1					$m_{H,S} \frac{S_S}{K_S+S_S} \frac{S_O}{K_O+S_O} X_H$
6. Maintenance on X_{STO}	−1						−1	$m_{H,STO} \frac{K_S}{K_S+S_S} \frac{S_O}{K_O+S_O} \frac{X_{STO}/X_H}{K_{STO}+(X_{STO}/X_H)} X_H$
7. Decay		$i_{NBM} - f_I i_{NXI}$		f_I	$1-f_I$	−1		$b_H \frac{K_S}{K_S+S_S} \frac{K_{STO}}{K_{STO}+(X_{STO}/X_H)} X_H$

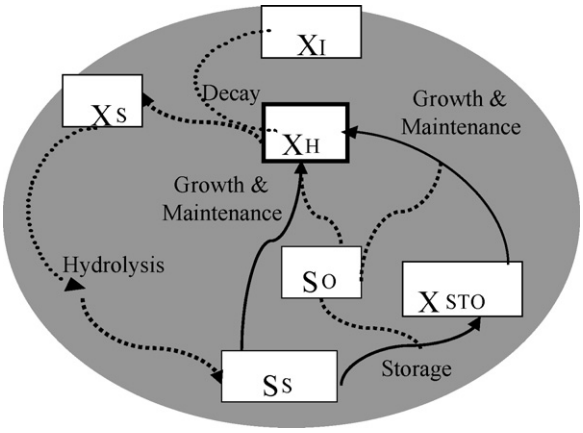

Fig. 1. Schematic framework illustrating the flow of the external and internal substrates in addition to the interactions among the involved components.

substrate within the cell in a polymeric form (polyhydroxybutyrate and/or glycogen) and growing on the external substrate. These stored materials are then consumed for growth and cell [11–12] when the external substrate becomes depleted. According to the anoxic simultaneous storage and growth concept, DO is consumed via the storage of the external substrate as internally stored materials, utilization of both external and internally stored materials for cell growth.

Modeling simultaneous storage and growth consists of two distinct but complementary phases: feast and famine (Fig. 1). Under feast conditions, based on a conventional ASM-type model structure, three distinctive yield coefficients independent from each other are used for storage (Y_{STO}), direct growth on the external substrate ($Y_{H,S}$) and growth on the internally stored products ($Y_{H,STO}$), respectively [5,7,10]. Under famine conditions, the degradation of the storage polymers is the rate-limiting step and it governs the growth rate [9].

The slowly biodegradable substrate is hydrolyzed at a rate governed by surface reaction kinetics (Eq. (1)). Hydrolysis process is presumably a rate-limiting step for further utilization of generated readily biodegradable substrate.

$$\frac{dX_S}{dt} = -k_H \frac{X_S/X_H}{K_X + (X_S/X_H)} X_H \tag{1}$$

Biomass growth and storage is defined by a hyperbolic Monod-type expression as commonly adopted in other models [1,9]. The growth stops when the external (S_S) and internal substrate (X_{STO}) are depleted by means of a substrate switch function controlled by the half saturation constant, K_S and K_{STO}, respectively. According to the model, when one unit of S_S is consumed for growth, its $Y_{H,S}$ fraction is converted into X_H and the remaining stoichiometric fraction $(1 - Y_{H,S})$ is used for energy, consuming an equivalent amount of dissolved oxygen, S_O.

The stoichiometry of the other two processes, storage of S_S as X_{STO} and growth on X_{STO}, are similar to that of growth on S_S. S_S is stored as X_{STO} with a stoichiometry of Y_{STO}. The remaining part $(1 - Y_{STO})$ is consumed as oxygen in the conversion of S_S. After the consumption of the external substrate, the internal storage polymer is consumed for cell growth. In the model matrix (Table 1), an inverse switch function is incorporated in order to activate X_{STO} consumption when S_S is exhausted. The processes of oxygen utilization rates for storage of S_S, growth on S_S and degradation of X_{STO} are formulated by following expressions.

$$\mathrm{OUR}_{\text{storage-S}} = \frac{1 - Y_{STO}}{Y_{STO}} k_{STO} \frac{S_S}{K_S + S_S} \frac{S_O}{K_{O_2} + S_O} X_H \tag{2}$$

$$\mathrm{OUR}_{\text{growth-S}} = \frac{1 - Y_{H,S}}{Y_{H,S}} \mu_{H,S} \frac{S_S}{K_S + S_S} \times \frac{S_O}{K_{O_2} + S_O} \frac{S_{NH_4}}{K_{NH_4} + S_{NH_4}} X_H \tag{3}$$

$$\mathrm{OUR}_{\text{growth-STO}} = \frac{1 - Y_{H,STO}}{Y_{H,STO}} \mu_{H,STO} X_H \frac{K_S}{K_S + S_S} \frac{S_O}{K_{O_2} + S_O} \times \frac{S_{NH_4}}{K_{NH_4} + S_{NH_4}} \frac{X_{STO}/X_H}{K_{STO} + (X_{STO}/X_H)} \tag{4}$$

Active microorganisms need maintenance energy for their activity and chemical processes. Maintenance is usually integrated into the substrate consumption rate by adding a maintenance coefficient (m) as follows [13]:

$$\frac{dS_S}{dt} = -\left(\frac{\mu}{Y} + m\right) X \tag{5}$$

In the model matrix (Table 1), Eq. (5) is divided into the process of growth and a substrate dependent maintenance process with a Monod term, which is significantly lower than that of growth. Maintenance is defined based on both external and internal substrates [14]. When S_S exists, S_S is consumed by X_H for their aerobic maintenance. As S_S becomes depleted, X_{STO} is consumed by X_H for their aerobic maintenance. These two maintenance kinetics rates $r_{\text{main-S}}$ and $r_{\text{main-STO}}$ are given below:

$$r_{\text{main-S}} = m_{H,S} X_H \frac{S_S}{K_S + S_S} \frac{S_O}{K_{O_2} + S_O} \tag{6}$$

$$r_{\text{main-STO}} = m_{H,STO} X_H \frac{K_S}{K_S + S_S} \frac{S_O}{K_{O_2} + S_O} \times \frac{X_{STO}/X_H}{K_{STO} + (X_{STO}/X_H)} \tag{7}$$

Eq. (8) describes the accumulation of particulate inert COD (X_I) as a result of decay of active biomass.

$$\frac{dX_I}{dt} = f_I b_H \frac{K_S}{K_S + S_S} \frac{K_{STO}}{K_{STO} + (X_{STO}/X_H)} X_H \tag{8}$$

The gas–liquid oxygen transfer rate is assumed to be proportional to the difference in the oxygen concentrations between gas and liquid interface, and the proportionality factor is volumetric oxygen transfer coefficient $k_L a$ [15]. It follows a mass balance equation below:

$$\frac{dS_O(t)}{dt} = k_L a (S_O^* - S_O(t)) \tag{9}$$

where S_O^* is the maximum oxygen solubility in liquid phase, and S_O is the oxygen concentration on granule surface, equal to

that in the bulk liquid because the liquid–solid oxygen transfer resistance is ignored.

3. Model calculation

A computer program, AQUASIM 2.0 [16], is used for modeling the biological processes in activated sludge. AQUASIM 2.0 is a useful program designed mainly for estimating the coefficients and parameters involved in bioreactor models. This program offers flexible definition of the kinetic model, flow scheme, and process control strategies; it also provides support for graphic display of the support of the simulation results, corresponding experimental data, and communication with spreadsheet programs [16].

4. Sensitivity analysis

The established model has a more complex carbon dynamics than ASM3 and its response may be influenced by the values of the new parameters. Prior to model calibration, a sensitivity analysis should be conducted to evaluate the most important parameters [17,18]. The determination of key parameters in the calibration process is dependent on the sensitivity of the model output to these parameters [19]. For a parameter to be reliably determined, the measured data should be highly sensitive to the changes of this parameter. A low sensitivity indicates that it is difficult to assign a unique value to the given parameter [16].

A sensitivity analysis using AQUASIM is performed to test the reliability of the parameter estimates. The following "absolute–relative" sensitivity function is used [16].

$$\delta_{yp}^{\mathrm{ar}} = p\,\frac{\partial y}{\partial p} \tag{10}$$

where $\delta_{yp}^{\mathrm{ar}}$ is the sensitivity analytical output to a model parameter, y is an arbitrary value related to a model variable (e.g., OUR or COD) calculated by AQUASIM, and p is a model parameter (e.g., $Y_{\mathrm{H,S}}$ or K_{STO}).

The function measures the absolute change of y for a 100% change in p. The positive sign of the function indicates that y increases with the increasing value of p, while the negative sign of the function indicates that y decreases with the increasing value of p. The sensitivity analysis involves all the kinetic and stoichiometric parameters in the established model. The sensitivities of the measured variables, i.e., OUR and COD in this work, to changes of these parameters are determined and shown in Figs. 2–5.

4.1. Effect of hydrolysis parameters

The effect of hydrolysis process parameters on the model outputs, the maximum hydrolysis rate (k_{H}) and hydrolysis affinity constant (K_{X}), is shown in Fig. 2. The sensitivity analytical results reveal that the dependence of OUR on the two parameters, k_{H} and K_{X}, leads to a similar shape of the changes in OUR just with a different sign and magnitude. This means that the variation induced by a change in k_{H} can be approximately balanced by appropriate changes in the parameter K_{X}. This makes

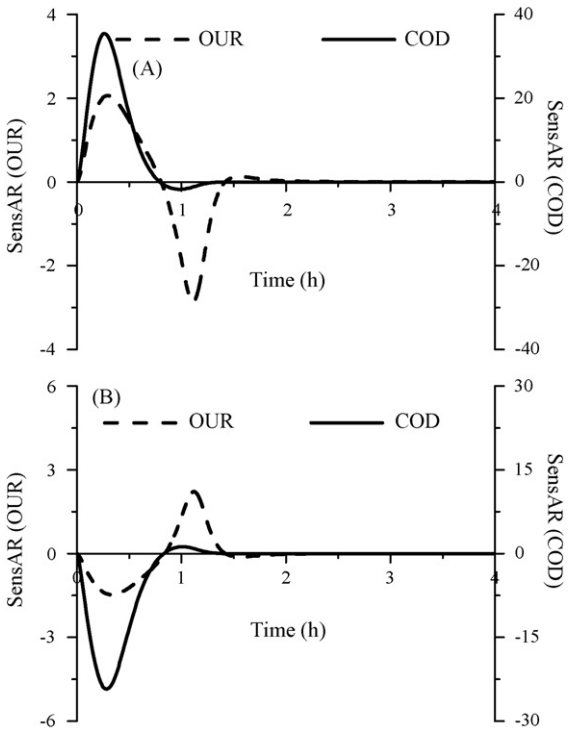

Fig. 2. Sensitivities (absolute–relative) of the measured signals (OUR and COD) to the hydrolysis process parameters [sensitivity vs. time (h)]: (A) k_{H}; (B) K_{X}.

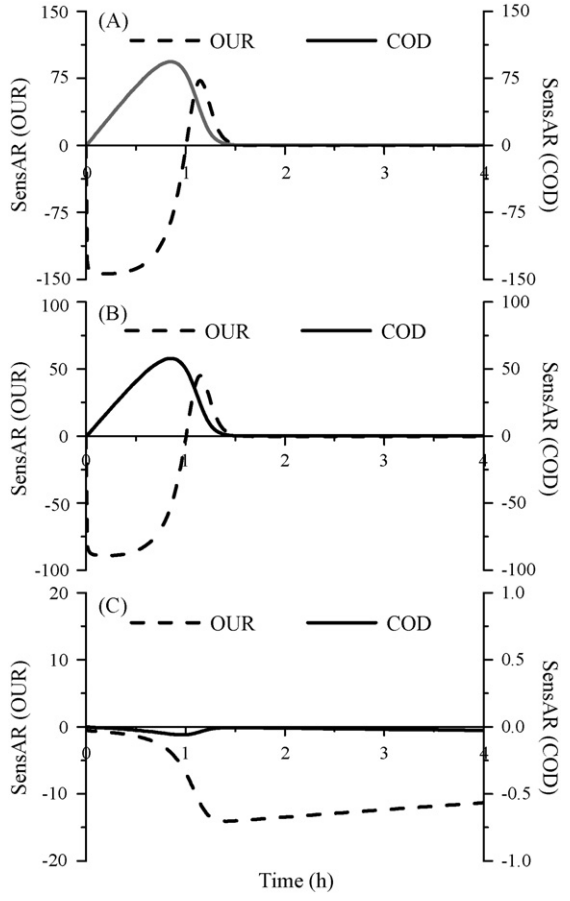

Fig. 3. Sensitivities (absolute–relative) of the measured signals (OUR and COD) to the stoichiometric parameters [sensitivity vs. time (h)]: (A) Y_{STO}; (B) $Y_{\mathrm{H,S}}$; (C) $Y_{\mathrm{H,STO}}$.

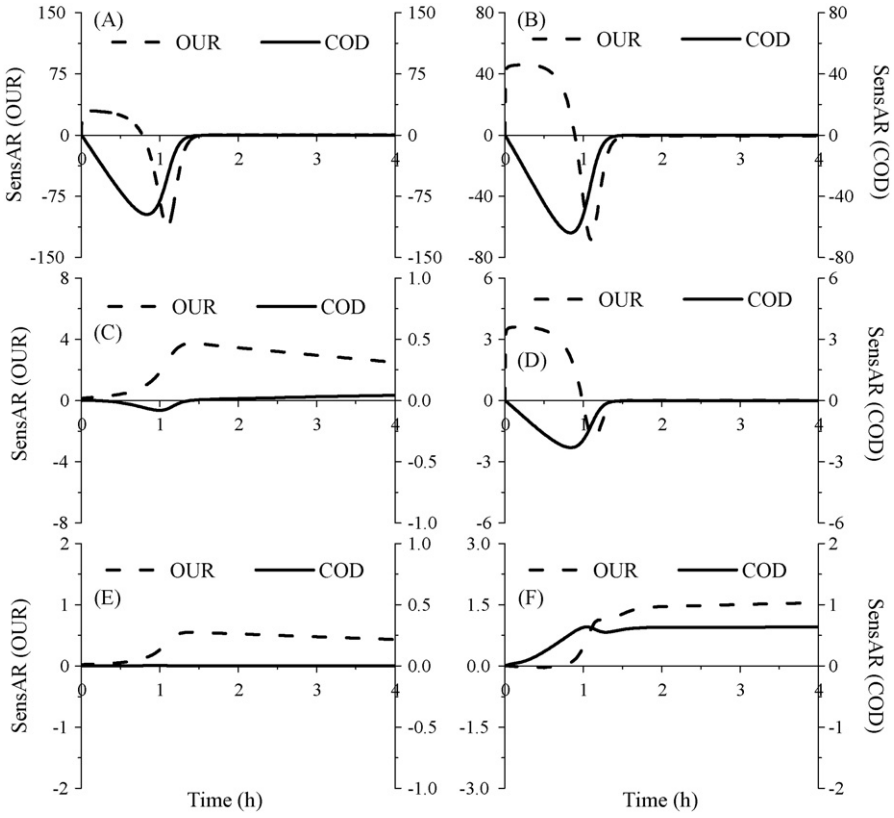

Fig. 4. Sensitivities (absolute–relative) of the measured signals (OUR and COD) to the kinetic parameters [sensitivity vs. time (h)]: (A) k_{STO}; (B) $\mu_{H,S}$; (C) $\mu_{H,STO}$; (D) $m_{H,S}$; (E) $m_{H,STO}$; (F) b_H.

these two parameters non-identifiable from the measured OUR data.

The dependence of COD on the two parameters k_H and K_X also has a similar changing pattern to COD with a different sign and magnitude. Since the sensitivity functions of COD lead to the same results (i.e., similar behavior of the sensitivity functions with respect to the parameters), these parameters cannot be resolved with the measured COD data only. The reason for the non-identifiability of the parameters to OUR and COD is that neither DO nor COD are consumed by the hydrolysis processes.

4.2. Effect of stoichiometric parameters

Storage of the readily biodegradable substrates under aerobic conditions plays an important role in the substrate removal. Meanwhile, the heterotrophic growth on the external substrate and the storage polymers has a considerable influence on the oxygen consumption. In this model, three distinctive yield coefficients independent from each other are used for storage (Y_{STO}), direct growth on the external substrate ($Y_{H,S}$) and growth on the internal storage polymers ($Y_{H,STO}$). These yield coefficients have a significant influence on the output variables (Fig. 3).

The dependence of OUR on Y_{STO} and $Y_{H,S}$ yields a similar shape of the OUR changes with a different magnitude. The dependence of OUR on $Y_{H,STO}$ is different from that on Y_{STO} and $Y_{H,S}$. The sensitivity of OUR with respect to Y_{STO} and $Y_{H,S}$ has its maximum at the very beginning and decreases exponentially, while the sensitivity of OUR with respect to $Y_{H,STO}$ increases from zero to its maximum value, but then decreases slightly. This makes these parameters identifiable from the OUR data. The dependence of COD on Y_{STO} and $Y_{H,S}$ also results in a similar shape with a different magnitude. COD is insensitive to the parameter $Y_{H,STO}$. This is reason the growth on X_{STO} does not affect the effluent COD concentration remarkably.

4.3. Effect of kinetic parameters

The sensitivity of kinetic parameters is shown in Fig. 4. The kinetic parameters k_{STO} and $\mu_{H,S}$ have a significant influence on the OUR output. The dependence of OUR on k_{STO} and $\mu_{H,S}$ leads to a similar shape of the OUR changes with a different but great magnitude. The dependence of OUR on $m_{H,S}$ also exhibits a similar shape of the OUR changes but with a much lower magnitude, compared to k_{STO} and $\mu_{H,S}$. The reason behind this is that the kinetic structures for the three processes (storage, growth on S_S and maintenance on S_S) in this model are almost the same, only with the different maximum rate values. It is evident that the parameters k_{STO} and $\mu_{H,S}$ are identifiable from the measured OUR, because for small values of the time, t, the calculated OUR is only sensitive to these two kinetic parameters.

The dependence of OUR on $\mu_{H,STO}$ and $m_{H,STO}$ are different from that on k_{STO} and $\mu_{H,S}$, the sensitivity of OUR with respect to $\mu_{H,STO}$ and $m_{H,STO}$ increases from zero, reaches a maximum and then decreases gradually. With the relative greater shape magnitude, $\mu_{H,STO}$ is also identifiable from the measured OUR. The sensitivity of OUR with respect to b_H is different from that

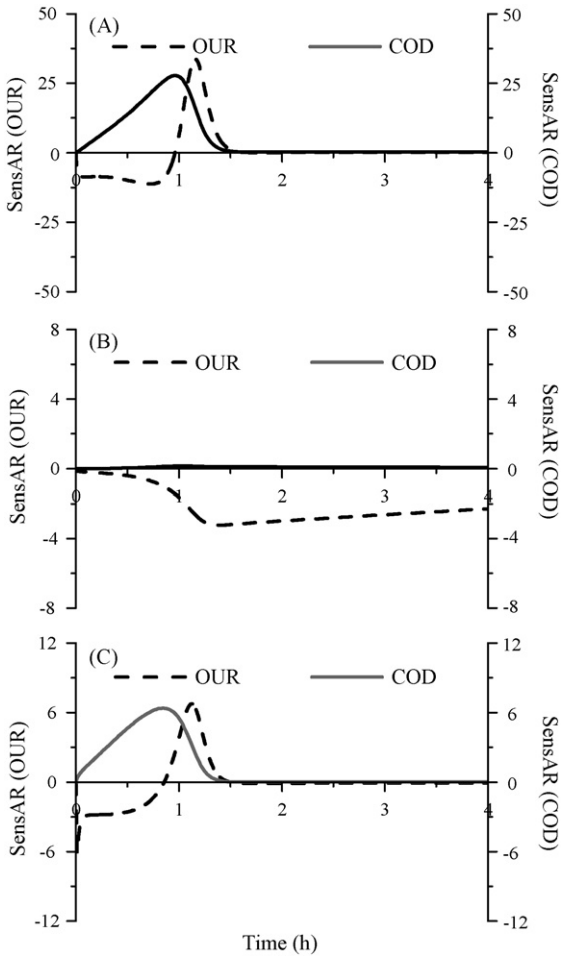

Fig. 5. Sensitivities (absolute–relative) of the measured signals (OUR and COD) to the affinity constant parameters [sensitivity vs. time (h)]: (A) K_S; (B) K_{STO}; (C) K_O.

for other kinetic parameters. There have similar results for the sensitivity of COD with respect to parameters k_{STO}, $\mu_{H,S}$, $m_{H,S}$ and b_H (Fig. 4). However, COD is insensitive to the parameters $\mu_{H,STO}$ and $m_{H,STO}$. This is because that the growth and maintenance on X_{STO} processes do not significantly affect the effluent concentration of COD in this model.

4.4. Effect of key affinity constant

Sensitivity of the three affinity constants (K_S, K_{STO}, and K_O) to the model outputs is tested and shown in Fig. 5. The dependence of OUR and COD on K_S and K_O leads to a similar changing shape. With an increase in K_S and K_O, the effluent COD increases initially, but decreases later. The dependence of OUR on K_{STO} increases from zero and reaches a maximum, but then decreases gradually. COD is insensitive to the parameter K_{STO}.

5. Model calibration

Model calibration procedure is a process of adjusting coefficient values of the model, so that the results simulated by the model with these coefficients closely agree with the measured data. The parameter values are estimated by minimizing the sum of squares of the deviations between the measured data and the model predictions with the objective function given as below [20]:

$$F(p) = \left(\sum_{i=1}^{n} (y_{\exp,i} - y(p)_i)^2 \right)^{1/2} \quad (11)$$

where y_{exp} and $y(p)$ are vectors of n measured values and model predictions at times t_i (i from 1 to n), and p is the vector of the model parameters. The standard deviation for parameter determination was required to be lower than 50% to ensure the validity of the values of the parameters obtained.

To initiate the calibration procedure, an initial guess of the parameters is necessary. Such initial values are obtained with the data in the literatures as shown in Table 2. To simplify the calibration process, it is desired to change as few constants as possible [21], because of the limited variability of some parameters. Four parameters, k_{STO}, $\mu_{H,STO}$, $\mu_{H,S}$, and K_S, are changed based on the causality of the parameters on the experimental data. In this study, the model is calibrated for the OUR, COD removal, and the internal storage polymer concentration. The selection of the parameters for calibration is mainly based on the result of sensitivity analysis.

6. Model evaluation

The model evaluation is performed from the comparison between the measured and calculated results. The experimental data of four related case studies shown in Table 3 are used for model evaluation. It should be noted that different wastewater characteristics, reactor operating conditions and microbial communities may result in a very wide variation of the obtained parameter values (as shown in Table 3). The model parameters are highly dependent on operating conditions.

6.1. Case 1: Model evaluation with experimental data of this study

Activated sludge are cultivated in a laboratory-scale sequencing batch reactor (SBR), which has a working volume of 2 L with an internal diameter of 7.0 cm and a height of 100 cm. It is operated sequentially as, 3 min of influent filling, 212 min of aeration, 15 min of settling and 10 min of effluent withdrawal. An air velocity of 0.4 $m^3\ h^{-1}$ is applied to the reactor, equivalent to a superficial upflow velocity of 2.8 $cm\ s^{-1}$. The SBR is fed with a fatty-acids-rich wastewater, which is the effluent of a laboratory-scale acidogenic reactor fed with sucrose-rich wastewater [22]. Butyrate, acetate and ethanol are its main constituents. Sodium bicarbonate of 100 $mg\ L^{-1}$ is introduced to the wastewater to provide buffering capacity in order to maintain the pH at 7.0.

The results are shown in Fig. 6. Four model parameters are calibrated in model simulation, and the values are shown in Table 3. The model simulation results agree with the experimental data well (Fig. 6). A tailing-off of the DO-consumption curve is observed in the respiration tests (Fig. 6A). This phenomenon

Table 2
Prameters used in the developed model (20 °C)

Parameter	Definition	Values	Unit	Reference
Stoichiometry				
Y_{STO}	Yield coefficient for storage	0.80	g COD g^{-1} COD	Sin et al. [9]
$Y_{H,S}$	Yield coefficient for growth on S_S	0.57	g COD g^{-1} COD	Sin et al. [9]
$Y_{H,STO}$	Yield coefficient for growth on X_{STO}	0.68	g COD g^{-1} COD	Sin et al. [9]
f_I	Fraction of X_I in decay	0.2	g COD g^{-1} COD	Gujer et al. [3]
i_{NBM}	Nitrogen content of biomass	0.07	g N g^{-1} COD	Gujer et al. [3]
i_{NXI}	Nitrogen content of X_I	0.02	g N g^{-1} COD	Gujer et al. [3]
Kinetics				
k_{STO}	Maximum storage rate of biomass	0.084	h^{-1}	Sin et al. [9]
$\mu_{H,STO}$	Maximum growth rate on X_{STO}	0.04	h^{-1}	Sin et al. [9]
$\mu_{H,S}$	Maximum growth rate on S_S	0.04	h^{-1}	Sin et al. [9]
K_S	Substrate affinity constant	2.0	g COD m^{-3}	Gujer et al. [3]
K_{STO}	Biomass affinity constant for X_{STO}	1.0	g COD g^{-1} COD	Gujer et al. [3]
K_O	Dissolve oxygen affinity constant	0.2	g COD m^{-3}	Gujer et al. [3]
$m_{H,S}$	Maintenance coefficient on S_S	0.0066	h^{-1}	Beun et al. [12]
$m_{H,STO}$	Maintenance coefficient on X_{STO}	0.0044	h^{-1}	Beun et al. [12]
b_H	Decay rate coefficient	0.0083	h^{-1}	Gujer et al. [3]
k_H	Maximum hydrolysis rate	0.125	h^{-1}	Gujer et al. [3]
K_X	Hydrolysis affinity constant	1	g COD g^{-1} COD	Gujer et al. [3]
K_{NH_4}	Biomass NH_4 affinity constant	0.01	g N m^{-3}	Gujer et al. [3]

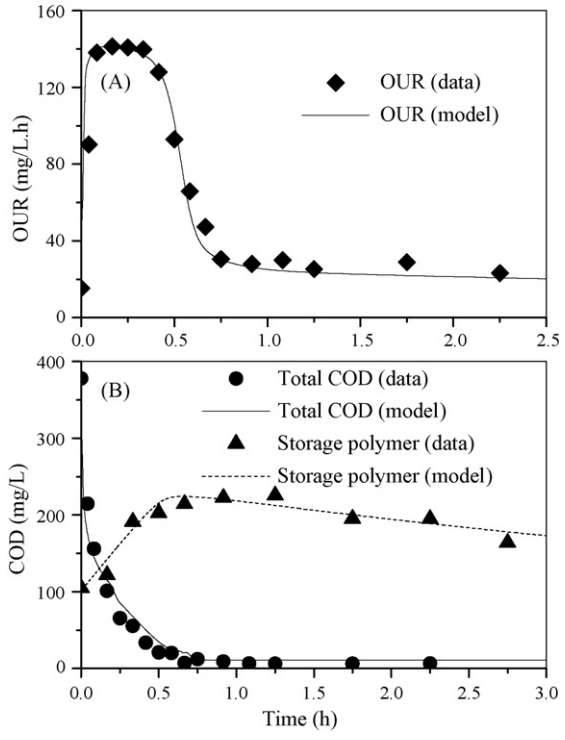

Fig. 6. Model evaluation of the experimental data of this study: (A) OUR profiles; (B) COD and storage polymer concentrations.

can be described with the model established in this work, in which simultaneous storage, growth and maintenance–decay are taken into account. The present model is able to predict both initial OUR response and smooth transition to the famine phase. The production of the storage polymers after a pulse addition of substrate and growth on the internally accumulated storage polymers after the depletion of the external substrate are also simulated. Two distinct phases can be observed (Fig. 6B). The first phase is the storage polymer production: a rapid uptake of substrate which is used for growth and storage polymer production. The next phase is the storage polymer consumption: after the depletion of the external substrate, growth on the accumulated storage polymer occurs. Furthermore, the COD profile is also well simulated (Fig. 6B).

The substrate affinity constants, K_S, are found to be in the same order of magnitude of the values obtained from other studies [1,7,9–10]. The initial high amount of readily biodegradable substrate results in a relatively rapid storage process with a maximum rate, k_{STO}, of 0.19 h^{-1}. The growth rates on storage polymers at famine phase ($\mu_{H,STO}$) is estimated to be 0.22 h^{-1} with a K_{STO} value of 1.0 g COD g^{-1} COD. These model results are in favor of a rapid substrate storage accompanied by an optimized primary growth on the available substrate, when excess substrate is present in the system [10].

The model validation results are given in Fig. 7 with the experimental data which are not previously used for model cali-

Table 3
Parameter values of the four cases for model evaluation

Cases	k_{STO} (h^{-1})	$\mu_{H,STO}$ (h^{-1})	$\mu_{H,S}$ (h^{-1})	K_S (g COD m^{-3})
This study	0.19	0.22	0.045	35.81
Krishna and van Loosdrecht [5]	0.048	0.16	0.054	0.24
Beun et al. [12]	7.40	0.42	0.54	12.31
Dionisi et al. [23]	0.034	0.43	0.11	0.017

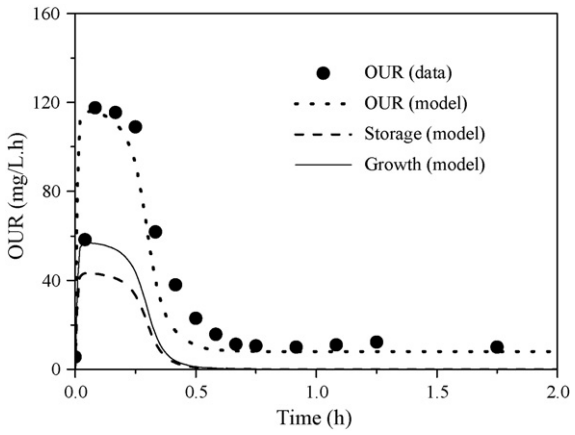

Fig. 7. Model validation using the measured OUR data of this study and the OUR fractions for simultaneous storage and growth calculated from the established model.

bration. The simulation results are satisfactory. Fig. 7 also shows the model interpretation of the OUR profiles according to Eqs. (2) and (3). A relatively high amount of substrate is used for primary growth, but a relatively low amount of substrate is utilized for storage. The validity of the model confirms that the consumption of DO, the removal and utilization of substrate, and the production and consumption of storage polymers under aerobic conditions can be well simulated by this model.

6.2. Case 2: Model evaluation with experimental data of Krishna and van Loosdrecht [5]

Model simulation is performed with the experimental data of Krishna and van Loosdrecht [5], who fed a laboratory-scale SBR with acetate as the sole substrate. The experiments were conducted in a 2-L double jacketed SBR equipped with pH, O_2 and redox-electrodes. The SBR was operated with a cycle of 4 h consisting of six process operation phases, resulting in a feast phase of 55 min and a famine phase of 185 min. To prevent the influence of nitrification on the measurements, allylthiourea was added at a concentration of 100 mg L^{-1}. Simulation is performed with the model and the parameter values are shown in Table 3. The measured and simulated results of the storage polymer and OUR profiles in one cycle are shown in Fig. 8 (symbols and line). Two distinct phases can be observed. During the feast phase, substrate (acetate) was used for growth, poly-β-hydroxybutyrate (PHB) formation and maintenance. During the famine phase, PHB was consumed for maintenance and growth. The established model captures all these components variation trends and gives a reasonable description of the storage and growth processes.

6.3. Case 3: Model evaluation with experimental data of Beun et al. [12]

The PHB metabolism in activated sludge cultures was studied by Beun et al. [12]. The activated sludge in a 2-L SBR was subjected to repeated feast and famine conditions, resulting in the storage and consumption of PHB in activated sludge. The calibrated parameter values are given in Table 3, and the simulated and measured acetate and PHB profiles are shown in Fig. 9. The validity of the present model is verified with acetate and PHB data in the experiment. When acetate was present, a linear decrease in acetate and a linear increase in PHB were measured and simulated. After the depletion of acetate, the PHB concentration slowly decreased to its initial level at the cycle beginning. In the feast period, 66–100% of the substrate consumed was used for PHB storage, the remaining was used for growth and maintenance. The model provides a relatively accurate prediction of PHB production and consumption. This confirms the validity of the established model again.

6.4. Case 4: Model evaluation with experimental data of Dionisi et al. [23]

Glutamic acid removal in activated sludge process was studied by Dionisi et al. [23]. Glutamic acid was used as the sole carbon source in the batch tests, and nitrification was inhibited through addition of thiourea at 20 mg L^{-1} in the feed. Measured and simulated profiles for glutamic acid (COD), storage polymer, and OUR in a batch test are shown in Fig. 10. Four model parameters are calibrated and the values are shown in Table 3. A good agreement between the measured and predicted results is achieved (Fig. 10), suggesting the validity of the model. PHB storage and biomass growth occurred simultaneously. After the addition of glutamic acid, it started to be removed, PHB was stored, and the OUR increased rapidly with respect to an initial low value. Later, glutamic acid was removed at an increasing rate, and correspondingly the PHB storage rate and OUR also

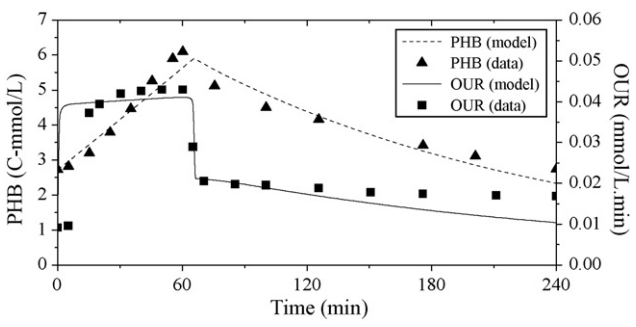

Fig. 8. Simulation results of the experimental data of Krishna and van Loosdrecht [5] for the PHB and OUR profiles.

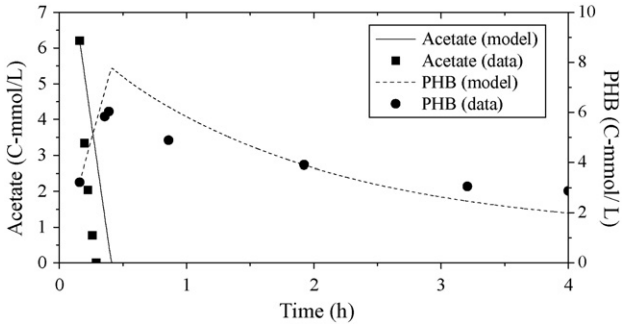

Fig. 9. Model evaluation of experimental results of Beun et al. [12] for acetate and PHB concentrations.

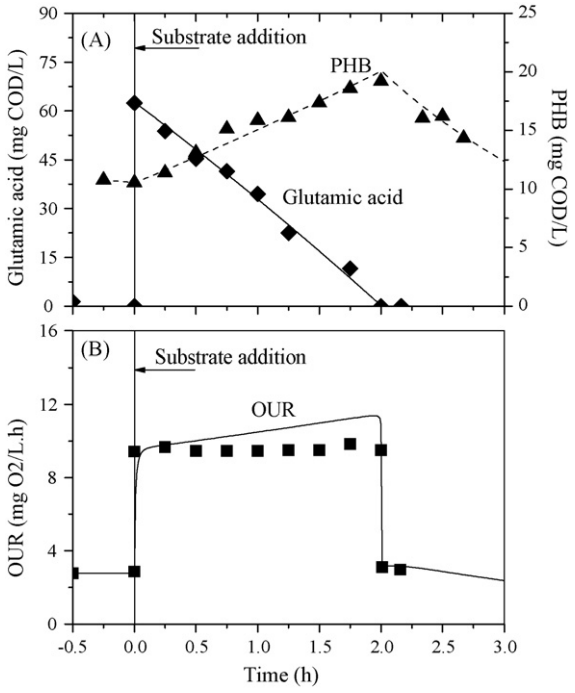

Fig. 10. Model evaluation of experimental results of Dionisi et al. [23] for the concentration profiles of: (A) glutamic acid and PHB; (B) OUR.

increased. When glutamic acid became depleted, PHB started to decrease, as it was utilized as an internal carbon source. Correspondingly, the OUR decreased markedly. Model verification results in this case also demonstrate that the present model is able to properly simulate the storage and growth processes in activated sludge.

7. Conclusions

In this study a generalized mathematic model based on an extension of ASM3 is developed to describe the simultaneous heterotrophic storage and growth processes in activated sludge under aerobic conditions, with a consideration of microbial maintenance and oxygen transfer. Microorganisms in activated sludge subjected to alternative feast and famine environments are able to take up the substrate rapidly and to store it as intracellular storage products when the substrate is in excess. The sensitivities of the measured variables (OUR and COD) to changes in key model parameters are analyzed. Four parameters (i.e., k_{STO}, $\mu_{H,STO}$, $\mu_{H,S}$, and K_S) are considered for the analysis based on their anticipated impact on the model output. The experimental results from four different case studies are used for model evaluation. The established model demonstrates its capacity of elucidating the simultaneous heterotrophic storage and growth processes in activated sludge under aerobic conditions.

Acknowledgements

The authors wish to thank the Natural Science Foundation of China (Grants 20577048 and 50625825), and the NSFC-RGC Joint Project (Grant 50418009) for the partial support of this study.

References

[1] M. Henze, W. Gujer, T. Mino, M.C.M. van Loosdrecht, Activated Sludge Models ASM1, ASM2, ASM2d, and ASM3, IWA Scientific and Technical Report No. 9, IWA Publishing, London, UK, 2000.
[2] M. Henze, C.P.L. Grady Jr., W. Gujer, G.V.R. Marais, T. Matsuo, Activated Sludge Model No. 1. Scientific and Technical Report No. 1, IAWPRC, London, 1987.
[3] W. Gujer, M. Henze, T. Mino, M.C.M. van Loosdrecht, Activated Sludge Model No. 3, Water Sci. Technol. 39 (1999) 183–193.
[4] K.V. Gernaey, M.C.M. van Loosdrecht, M. Henze, M. Lind, S.B. Jorgensen, Activated sludge wastewater treatment plant modelling and simulation: state of the art, Environ. Model. Software 19 (2004) 763–783.
[5] C. Krishna, M.C.M. van Loosdrecht, Substrate flux into storage and growth in relation to activated sludge modelling, Water Res. 33 (1999) 3149–3161.
[6] A. Carucci, D. Dionisi, M. Majone, E. Rolle, P. Smurra, Aerobic storage by activated sludge on real wastewater, Water Res. 35 (2001) 3833–3844.
[7] S. Pratt, Z. Yuan, J. Keller, Modelling aerobic carbon oxidation and storage by integrating respirometric, titrimetric, and off-gas CO_2 measurements, Biotechnol. Bioeng. 88 (2004) 135–147.
[8] W. Gujer, T.A. Larsen, The implementation of biokinetics and conservation principles in ASIM, Water Sci. Technol. 31 (1995) 257–266.
[9] G. Sin, A. Guisasola, D.J.W. De Pauw, J.A. Baeza, J. Carrera, P.A. Vanrolleghem, A new approach for modelling simultaneous storage and growth processes for activated sludge systems under aerobic conditions, Biotechnol. Bioeng. 92 (2005) 600–613.
[10] O. Karahan, M.C.M. van Loosdrecht, D. Orhon, Modeling the utilization of starch by activated sludge for simultaneous substrate storage and microbial growth, Biotechnol. Bioeng. 94 (2006) 43–53.
[11] M.C.M. van Loosdrecht, M.A. Pot, J.J. Heijnen, Importance of bacterial storage polymers in bioprocesses, Water Sci. Technol. 35 (1997) 41–47.
[12] J.J. Beun, F. Paletta, M.C.M. Van Loosdrecht, J.J. Heijnen, Stoichiometry and kinetics of poly-β-hydroxybutyrate metabolism in aerobic, slow growing, activated sludge cultures, Biotechnol. Bioeng. 67 (2000) 379–389.
[13] H. Horn, D. Hempel, Growth and decay in an auto-/heterotrophic biofilm, Water Res. 31 (1997) 2243–2252.
[14] M.C.M. van Loosdrecht, M. Henze, Maintenance, endogenous respiration, lysis, decay and predation, Water Sci. Technol. 39 (1999) 107–117.
[15] C. Nicolella, M.C.M. van Loosdrecht, J.J. Heijnen, Mass transfer and reaction in a biofilm airlift suspension reactor, Chem. Eng. Sci. 53 (1998) 2743–2753.
[16] P. Reichert, AQUASIM 2.0—User Manual, Computer Program for the Identification and Simulation of Aquatic Systems, Swiss Federal Institute for Environmental Science and Technology (EAWAG), 1998.
[17] A.B. Shahalam, R. Elsamra, G.M. Ayoub, A. Acra, Parametric sensitivity of comprehensive model of aerobic fluidized-bed biofilm process, J. Environ. Eng.-ASCE 122 (1996) 1085–1093.
[18] A.E. Abasaeed, Sensitivity analysis on a sequencing batch reactor model. I. Effect of kinetic parameters, J. Chem. Technol. Biotechnol. 70 (1997) 379–383.
[19] G. Koch, M. Kuhni, W. Gujer, H. Siegrist, Calibration and validation of Activated Sludge Model No. 3 for Swiss municipal wastewater, Water Res. 34 (2000) 3580–3590.
[20] I. Jubany, J.A. Baeza, J. Carrera, J. Lafuente, Respirometric calibration and validation of a biological nitrite oxidation model including biomass growth and substrate inhibition, Water Res. 39 (2005) 4574–4584.
[21] S.L. Xu, B. Hultman, Experiences in wastewater characterization and model calibration for the activated sludge process, Water Sci. Technol. 33 (1996) 89–98.
[22] Y. Mu, H.Q. Yu, Biological hydrogen production in a UASB reactor with granules I: Physicochemical characteristics of hydrogen-producing granules, Biotechnol. Bioeng. 94 (2006) 980–987.
[23] D. Dionisi, M. Majone, A. Miccheli, C. Puccetti, C. Sinisi, Glutamic acid removal and PHB storage in the activated sludge process under dynamic conditions, Biotechnol. Bioeng. 86 (2004) 842–851.